Journal of Alloys and Compounds 472 (2009) 325–327

Contents lists available at ScienceDirect

Journal of Alloys and Compounds

journal homepage: www.elsevier.com/locate/jallcom

Synthesis and characterization of In_2S_3 nanoparticles

Guangxiu Cao [a], Yanbao Zhao [b,*], Zhishen Wu [b]

[a] Department of Chemistry, Shangqiu Normal College, Henan Shangqiu 476000, China
[b] Lab for Special Functional Materials, Henan University, Henan Kaifeng 475004, China

ARTICLE INFO

Article history:
Received 3 September 2007
Received in revised form 14 April 2008
Accepted 16 April 2008
Available online 27 May 2008

Keywords:
Preparation
In_2S_3 nanoparticles
Characterization
Optical property
Mechanism

ABSTRACT

In this paper, we report a novel solution route to prepare In_2S_3 nanoparticles through directly dispersing melted indium in a sulfur-dissolved solvent. X-ray powder diffraction (XRD), transmission electron microscopy (TEM) and electron diffraction (ED) show the formation of In_2S_3 nanoparticles possessing tetragonal structure with an average particle diameter of 30 nm. The as-prepared In_2S_3 nanoparticles display strong blue–UV emission, promising for applications in optical devices.

1. Introduction

Over the past decades, there has been increasing interest in III–VI materials due to their unique physical and chemical properties and potential applications in diverse areas [1]. Tetragonal In_2S_3, an III–VI chalcogenide, is an n-type semiconductor with a band gap of 2.00–2.20 eV, which has already inspired applications in optoelectronic, photovoltaic industries and solar cell devices [2,3]. Several physical and chemical methods have been developed to fabricate In_2S_3 with different morphologies [4,5]. For instance, a direct reaction of the elements in a quartz container at a high temperature [6], chemical deposition [7], heat treatment of In_2O_3 in H_2S at elevated temperatures [8], the metathesis reaction of $InCl_3$ and Li_2S [9], and wet chemical methods [10–12]. In_2S_3 nanoparticles represent an important class of materials that are potentially useful for a wide range of applications such as delivery vehicle systems, photonic crystals, fillers, and catalysts [13]. However, compared with In_2S_3 films and powder, much less work has been performed on In_2S_3 nanoparticles [14].

In previous papers, we have successfully produced metal nanoparticles by solution dispersion route in which the melting metal can be dispersed into nanosized droplets and converted into metal nanoparticles when the temperature is reduced to room temperature [15,16]. In this paper, we report a modified solution dispersion route to prepare In_2S_3 nanoparticles through one-step elemental reactions in paraffin oil.

2. Experimental

2.1. Chemicals and preparation

All materials were used without further purification. Indium granules (99.95%), sulfur powder (99.9%) and paraffin oil were analytical pure reagents from Shanghai Chemical Co., Shaoyang Chemical Co., and Luoyang Chemical Co., respectively. In a typical synthesis, 0.7 g commercial indium granules and 0.3 g sulfur powder were added to 40 mL of paraffin oil in a flask, and the system was sealed and stirred above 180 °C for at least 10 h. Then, the supernatant was cooled, centrifuged, washed with chloroform, and dried to get gray–black product.

2.2. Characterization

X-ray powder diffraction (XRD) was performed on an X'Pert Philips diffractometer equipped with Ni-filtered Cu Kα radiation (λ = 1.5418 Å) and operating at 40 kV and 40 mA. Transmission electron microscopy (TEM) was carried out on a JEOL JEM-2010Ex transmission electron microscope, with a tungsten filament at an acceleration voltage of 200 kV. Differential thermal analysis and thermogravimetry (DTA and TG) were conducted on the powders in the 30–500 °C temperature range, with an Exstar 6000 thermal system, a heating rate of 10 °C/min and in airflow. X-ray photoelectron spectra (XPS) were collected on an axis of ultra X-ray photoelectron spectrometer, and the XPS analyses were corrected with reference to C 1s (284.6 eV). The room-temperature photoluminescence (PL) spectrum was measured on a Spex F-212 fluorescence spectrophotometer with a Xe lamp upon excitation at 300 nm.

3. Results and discussion

3.1. XRD studies

Fig. 1 shows an XRD pattern of the In_2S_3 samples prepared by solution dispersion. The XRD pattern exhibits multiple intense peaks that are clearly distinguishable. All the reflection peaks can be

* Corresponding author.
E-mail address: zhaoyb902@henu.edu.cn (Y. Zhao).

0925-8388/$ – see front matter
doi:10.1016/j.jallcom.2008.04.047

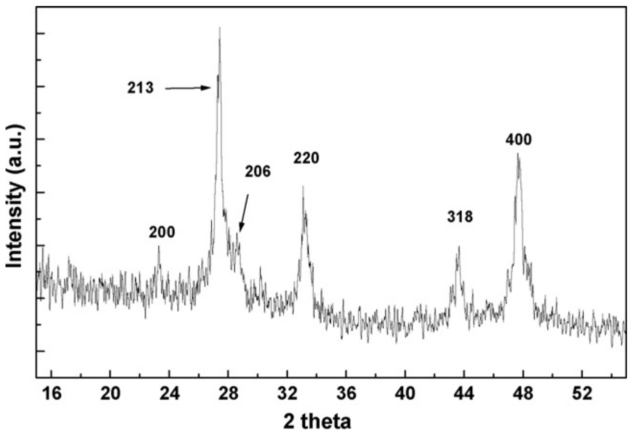

Fig. 1. XRD pattern of In_2S_3 nanoparticles prepared.

indexed to the tetragonal In_2S_3, and the peak positions are in good agreement with the known data (JCPDS: 33–1375). The refraction peaks represent different crystal planes, which are assigned to the crystal planes of [2 0 0], [2 1 3], [2 0 6], [2 2 0], [3 1 8], and [4 0 0] of crystalline In_2S_3, respectively, implying the formation of tetragonal In_2S_3.

3.2. TEM and ED studies

The morphology of the products was further examined by TEM. Fig. 2 displays a typical TEM image of as-prepared indium sulfide. It can be seen that the particles present broad size distribution with the average particle diameter of 30 nm. The large size distribution is naturally caused by the broad size distribution of the liquid indium droplets formed by stirring effect. Most particles appear to be nearly spherical shape. The corresponding electron diffraction (ED) pattern (inset) taken from a single In_2S_3 particle consists of regular diffraction spots, which reveals the single crystalline nature of the sample. The ED result is consistent with the XRD results presented above.

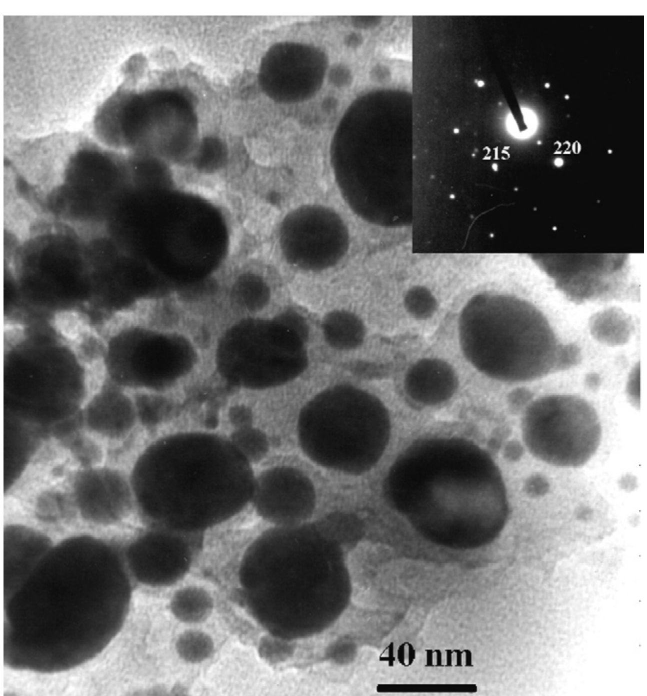

Fig. 2. TEM image and ED pattern (inset) of the as-obtained In_2S_3.

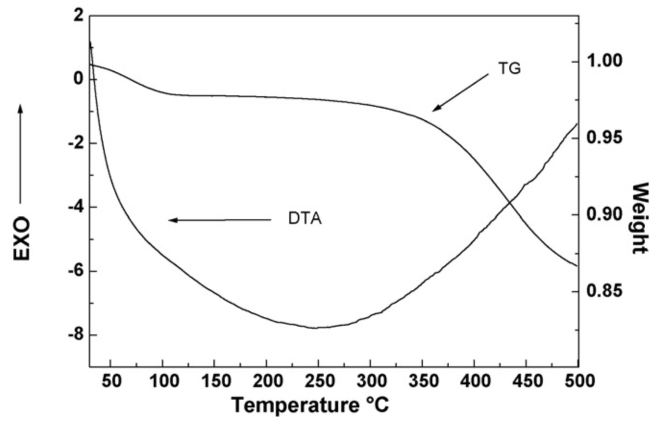

Fig. 3. TG/DTA curves of as-prepared In_2S_3 sample.

3.3. Thermal analysis

The thermal behavior of as-obtained product was investigated by DTA and TG in airflow. Fig. 3 gives the DTA/TG curves of as-obtained In_2S_3 product. It can be seen that the sample shows two distinct weight-loss steps in the temperature range of 30–500 °C on the TG curve. The first weight-loss process taking place below 100 °C can be attributed to the desorption of small molecules from the sample powder. The second mass loss (above 250 °C) might be assigned to the further releasing of solvent molecules or organic residuals in the samples. On the DTA curve, the product does not show the characteristic melting peak of metal In at 156 °C, which indicates that metal In is completely converted into indium sulfide.

3.4. XPS analysis

Further evidence for the quality and composition of the samples was obtained by the XPS of the products. The binding energies obtained in the XPS analysis were corrected for specimen charging by referencing the C 1s to 284.6 eV. The In 3d core level spectrum (Fig. 4a) shows the observed value of the binding energies for In $3d_{5/2}$ (444.8 eV) are in good agreement with those observed in $CdIn_2S_4$, which is indicative of indium as trivalent In^{3+} ions. The S_{2p} spectrum (Fig. 4b) appears a broad peak, which indicates that the particle surface sulfur might exist in form of S^{2-} (161.8 eV) and element S (163.8 eV). The contents of In and S are quantified by In 3d and S 2p peak areas, and a molar ratio of 1:1.52 for In:S is given. Thus, the XPS results further prove that the sample is composed of In_2S_3.

3.5. Proposed the mechanism for formation of In_2S_3 nanoparticles

According to the above analysis, the formation mechanism of In_2S_3 nanoparticles might be involving the dispersion of melting indium droplets, surface sulfuration of indium droplets, the diffusion of sulfur from the droplet surface to the inner, as well as solvent and sulfur adsorption at the droplet surface. A possible pathway for the formation of In_2S_3 nanoparticles might be as below. First, large indium droplets are dispersed into small droplets in solvent by stirring force; then, the fresh surface of indium droplet forms indium sulfide layer through reaction with sulfur dissolved in solvent, which should prevent the smaller droplets from coagulating, and the indium sulfide layer can adsorb efficiently solvent molecules to stabilize the droplets in solvent. With the presence of

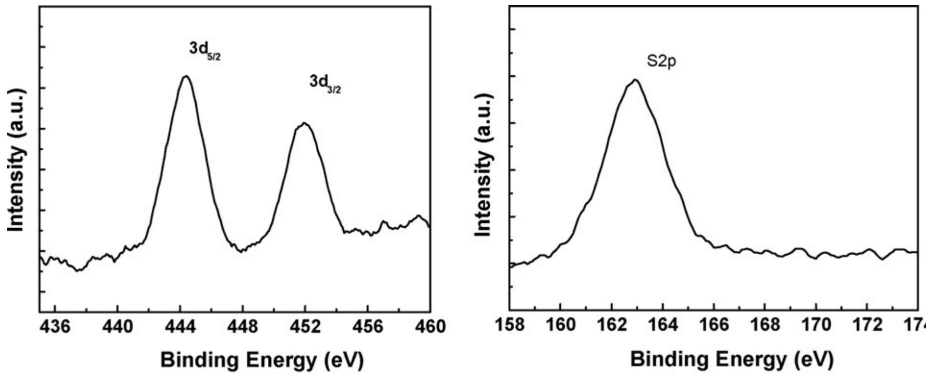

Fig. 4. XPS spectra of the In_2S_3 samples: (a) In 3d peak; and (b) S 2p peak.

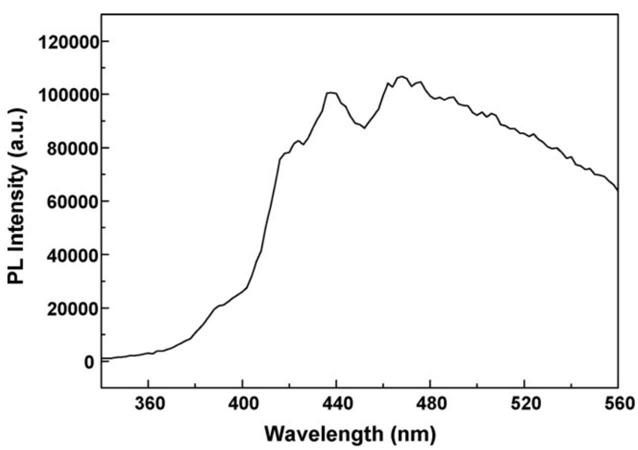

Fig. 5. PL spectrum of as-prepared In_2S_3 nanoparticles.

an indium sulfide layer, indium droplets should be further crushed into nanosized droplets. In addition, the indium sulfide layer should adsorb sulfur from solvent, which can diffuse to the inner droplet and provide the sulfur source required for the sulfuration of inner indium, resulting in the formation of In_2S_3 nanoparticles.

3.6. Optical properties

Fig. 5 shows the PL emission spectrum of the In_2S_3 nanoparticles dissolved in chloroform. The PL feature of In_2S_3 nanoparticles shows two strong and broad emission bands centered at 470 nm (blue emission) and 435 nm (UV emission), with two shoulders at 415 and 390 nm, respectively, which obviously reveals their blue shift compared with the reported data of 620.6 nm for In_2S_3 bulk materials. However, the Bohr radius of the excitation for In_2S_3 was known to be ~34 nm [14], hence, the UV emission may also be attributed to quantum-confined effects of In_2S_3 nanoparticles. Generally, the blue luminescence emission is mainly attributed to the existence of sulfur vacancies. These sulfur vacancies generally act as deep defect donors in semiconductors and would induce the formation of new energy levels in the band gap. The blue emission thus results from the radioactive recombination of a photoexcited hole with an electron occupying the sulfur vacancies. Since the nanoparticle sample contains a distribution of different sized particles, the larger particles that have smaller band gaps absorb and emit at longer wavelengths relative to smaller particles in the distribution [17]. In addition, the possibility of In_2O_3 presence should also favor the existence of surface defect sites. The very broad PL background signal seems to support this fact. The strong blue–UV emission also suggests that the In_2S_3 nanoparticles have potential to be a blue and a UV light emitter.

4. Conclusion

The In_2S_3 nanoparticles were prepared from metal indium and elemental sulfur via the solution dispersion, which might be suitable for many low melting point metals. The product through this technique is cheaper, and the surface properties of nanoparticles can be greatly modified by changing the composition of the solvent. The as-prepared In_2S_3 nanoparticles appear to be close to a spherical shape and have a good crystalline. The obtained In_2S_3 nanoparticles show strong blue–UV emission, promising for applications in optical devices.

Acknowledgements

This work was supported by National Science Foundation of China (NSFC) (No. 20671029) and Excellent Youth Foundation of Henan Province (No. 0612002900).

References

[1] P.M. Sirimanne, N. Sonoyama, T. Sakata, Chem. Phys. Lett. 350 (2001) 211.
[2] R. Nomura, S. Inazawa, K. Kanaya, H. Matsuda, Appl. Organomet. Chem. 3 (1989) 195.
[3] E. Dalas, L. Kobotiatis, J. Mater. Sci. 28 (1993) 5456.
[4] M.M. El-Nahass, B.A. Khalifa, H.S. Soliman, M.A.M. Seyam, Thin Solid Films 515 (2006) 1796.
[5] Y. Xiong, Y. Xie, G. Du, X. Tian, Y. Qian, J. Solid State Chem. 166 (2002) 336.
[6] N. Barreau, S. Marsillac, J.C. Bernede, Vacuum 56 (2000) 101.
[7] M.G. Sandoval-Paz, M. Sotelo-Lerma, J.J. Valenzuela-Jauregui, M. Flores-Acosta, R. Ramırez-Bon, Thin Solid Films 472 (2005) 5.
[8] P.M. Sirimanne, S. Shiozaki, N. Sonoyama, T. Sakata, Sol. Energy Mater. Sol. Cells 62 (2000) 247.
[9] J.C. Fitzmaurice, I.P. Parkin, Main Group Met. Chem. 17 (1994) 481.
[10] Y. Liu, M. Zhang, Y. Gao, R. Zhang, Y. Qian, Mater. Chem. Phys. 101 (2007) 362.
[11] Z.P. Ai, Opt. Mater. 24 (2003) 589.
[12] P.N. Kumta, P.P. Phule, S.H. Risbud, Mater. Lett. 5 (1987) 401.
[13] Y.R. Ma, L.M. Qi, J.M. Ma, H.M. Cheng, Langmuir 19 (2003) 4040.
[14] W. Chen, J.O. Bovin, A.G. Joly, S. Wang, F. Su, G. Li, J. Phys. Chem. B 108 (2004) 11927.
[15] Y.B. Zhao, Z.J. Zhang, H.X. Dang, J. Phys. Chem. B 107 (2003) 7574.
[16] Y.B. Zhao, Z.J. Zhang, H.X. Dang, Mater. Sci. Eng. A359 (2003) 405.
[17] W. Hoheisel, V.L. Colvin, C.S. Johnson, A.P. Alivisatos, J. Chem. Phys. 101 (1994) 8455.